Magnetic evolution of the amorphous and nanocrystalline phases and interphase coupling during the crystallization of $Fe_{87}Zr_6B_6Cu$: A ferromagnetic resonance study

D. S. Schmool,* J. S. Garitaonandia, and J. M. Barandiarán
Departamento de Electricidad y Electrónica, Facultad de Ciencias, Universidad del País Vasco/EHU, Apartado 644, E-48080 Bilbao, Spain
(Received 29 December 1997)

We present results of ferromagnetic resonance measurements on the alloy $Fe_{87}Zr_6B_6Cu$. These show the changes occurring in the sample, both magnetically and structurally, during the crystallization process. In this alloy the amorphous phase gradually crystallizes, forming nanocrystallites of α-Fe in a remaining ferromagnetic amorphous matrix. Results show evidence of a disordered and Fe-rich interphase region surrounding the Fe crystallites. This interphase region initially grows along with the growth of the Fe nanocrystals. However, in the latter stages of the Fe nanocrystallization, this phase also crystallizes into the Fe phase and other crystalline phases, and disappears at the end of the Fe crystallization and the beginning of second crystallization. Evidence of an interface localized spin wave mode at the boundary between the amorphous ferromagnetic and Fe phases in the early stages of crystallization is also observed. At higher annealing temperatures, we observe another resonance absorption feature. This is due to the onset of the second stage of crystallization, where FeZr and iron-boride phases form. The results of the ferromagnetic resonance are analyzed in a multiphase regime, where the importance of the magnetic coupling between the various magnetic phases is evident. A minimum of the in-plane anisotropy is found to coincide with the softest magnetic properties of this alloy. [S0163-1829(98)03441-9]

I. INTRODUCTION

The nanocrystalline state of amorphous alloys after partial devitrification by thermal annealing consists of small ultrafine crystallites surrounded by a remaining ferromagnetic amorphous matrix.[1–4] In the case of FeZrCuB, these small grains consist of α-Fe nanocrystals.[5–7] The excellent soft magnetic properties exhibited by these alloys, as well as other similar systems such as the finemets, are due to the fine microstructure of the small magnetic grains (or nanocrystallites) embedded in a ferromagnetic amorphous matrix. The small magnetic grains suppress local magnetocrystalline anisotropy due to exchange interactions.[2]

The technique of ferromagnetic resonance (FMR) is very powerful, allowing the magnetic characterization of materials. Primarily FMR is a magnetic measurement which allows the determination of bulk magnetic parameters, such as saturation magnetization, g factors, and magnetocrystalline anisotropy constants.[8] The linewidths of the resonance absorption peaks contain information about magnetic inhomogeneities and sample crystallinity as well as the intrinsic relaxation processes in magnetic samples.[8–11] In confined magnetic systems, which could be thin films or samples of a granular nature, it is possible to obtain further information regarding surface or interface anisotropies and the exchange stiffness parameter whereby we observe multipeaked spectra, due to resonance absorption by standing spin wave resonance modes.[12–14] In magnetic layered structures, ferromagnetic and spin wave resonance will allow the determination of the exchange coupling strength between adjacent magnetic layers.[15–17] In multiphase magnetic materials, such as mixed amorphous and nanocrystalline systems, we may expect a shift in the field positions of the resonance modes of the different phases due to the magnetic exchange coupling that exists between the various magnetic phases.[18] Other amorphous and nanocrystalline mixed phase alloys have been measured by ferromagnetic resonance.[19–21] By a careful study of the spectra we can obtain a high degree of information about the various magnetic phases in the sample and the changes that occur during the crystallization process.

In the present study we report on a detailed investigation of the crystallization process in $Fe_{87}Zr_6B_6Cu$ amorphous ribbons, which are produced by the melt-spinning technique, using ferromagnetic resonance. FMR offers a unique measurement of the magnetic properties of these alloys, as in this material the magnetic phases (α-Fe and amorphous phase) are of a very distinct nature which will give separable resonances in the FMR spectra. This will allow the observation of the changes (which are of both a structural and magnetic nature) in both magnetic phases as a function of the annealing treatment. It will be noted, however, that due to the strong magnetic exchange interaction between the phases, we expect a shift in the resonance field positions, and other effects, such as interface resonances. These materials exhibit a high-field resonance mode which has been interpreted as a spin wave resonance mode localized at the sample edges.[22] We show the importance of a magnetic multiphase approach to the interpretation of the FMR spectra, and the changes observed with crystallization.

II. EXPERIMENTAL

Samples of rectangular shape with a cross section of 1 mm by 20 μm prepared from amorphous ribbons, with composition $Fe_{87}Zr_6B_6Cu$, have been studied. These ribbons

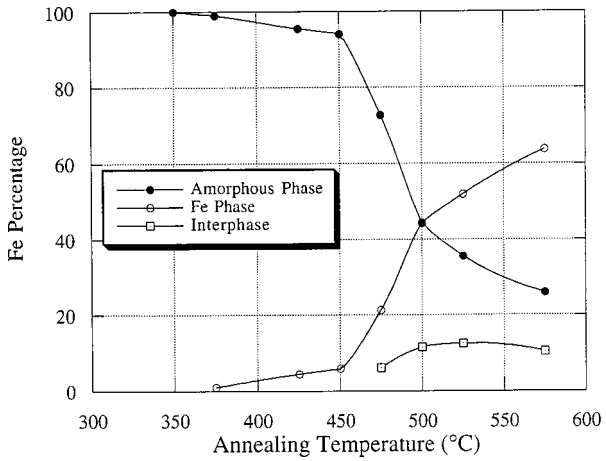

FIG. 1. Percentages of phases present in the sample as a function of the annealing temperature, taken from Mössbauer spectroscopy (Ref. 23).

were produced by the melt-spinning technique in a controlled environment. The annealing of these samples was performed isochronally at a preset temperature for 1 h under an argon atmosphere, in the temperature range 350–650 °C.

The ferromagnetic resonance experiments were performed at room temperature with a fixed microwave frequency of ~9.5 GHz, in a Bruker EPR spectrometer, in the Magnetic Measurement Services of the University of the Basque Country. FMR measurements were performed on the samples at various stages in the crystallization process, from the as-quenched state to an annealing temperature of 650 °C. The samples were mounted in the measuring cavity such as to allow in-plane measurements, i.e., where the applied static magnetic field is in the sample plane and the magnetic component of the microwave field varying in the direction of the sample normal. The sample was placed on a rotatable sample holder, which allows a variation of the external applied field with respect to the sample, with an accuracy of less than 0.5°. In this manner the angle of the applied field was varied in the sample plane from 0° to 180° at 10° intervals. In these measurements 0° corresponds to a direction along the direction of the ribbon and 90° is the direction across the ribbon.

III. RESULTS

In Fig. 1 we show the percentages of Fe in the various magnetic phases as a function of the annealing temperature. This data has been taken from Mössbauer spectroscopy, see Ref. 23. This shows the reduction of the amorphous phase content as the α-Fe phase grows. Above 450 °C, we also observe the appearance of an interphase region, which has a magnetically distinct behavior from that of the amorphous and crystallized Fe phases. The interphase is highly disordered and Fe rich. The quantity of this phase initially increases to a maximum of around 12.5% of the total Fe content at an annealing temperature of 525 °C, and then decreases as it gradually crystallizes into the various crystalline phases during second crystallization.

Figure 2 shows the ferromagnetic resonance spectra for the samples at various stages in the crystallization process, where spectra are shown for the along ribbon direction [$\phi = 0°$, Fig. 2(a)] and the across ribbon direction [$\phi = 90°$, Fig. 2(b)]. In the as-quenched state, the resonance signal will clearly arise from only a single amorphous magnetic phase. This is very clear in the spectrum at $\phi = 0°$. However, in the $\phi = 90°$ spectrum there are several other resonance features apart from the main FMR line at about 1800 Oe. At the low

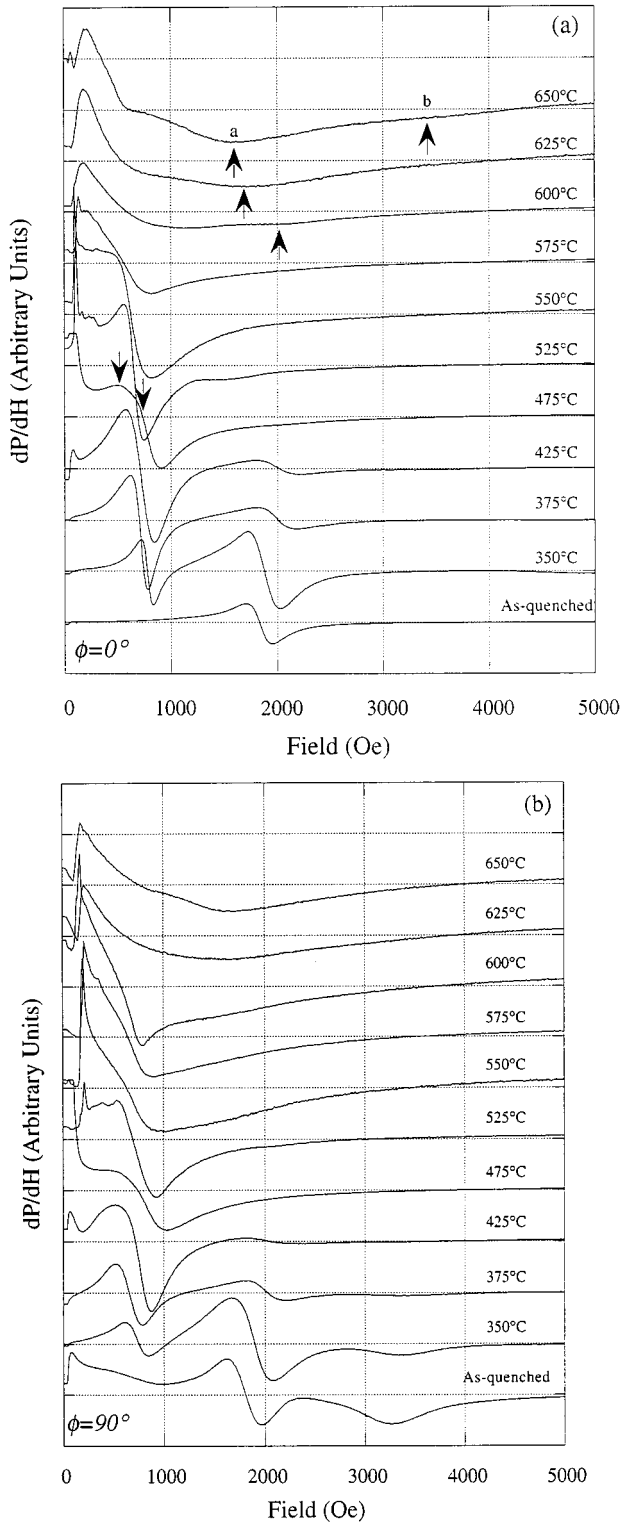

FIG. 2. Ferromagnetic resonance spectra as a function of the annealing temperature, indicated for each spectrum, for (a) along ribbon, $\phi = 0°$, (a and b denote the appearance of the phases Fe_2B and Fe_3Zr, respectively, see text) and (b) across ribbon, $\phi = 90°$, geometries.

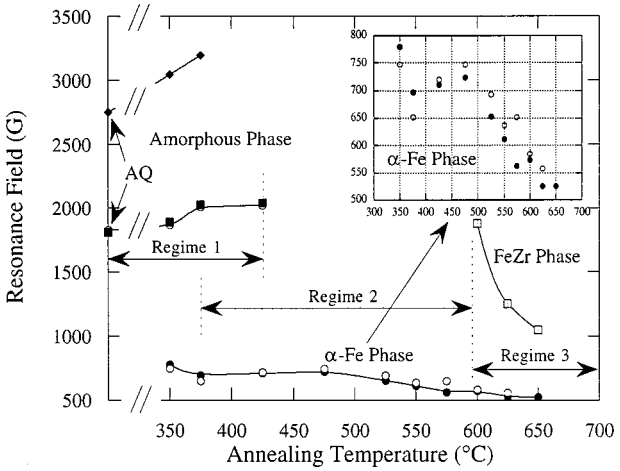

FIG. 3. Resonance field position versus annealing temperature. AQ denotes the as-quenched state. The inset shows an expanded view of the variation of the resonance field for the Fe phase resonance. We also indicate the three annealing temperature regimes used in the analysis, see text.

field end of the spectrum there is a resonance feature at about 100 Oe, this is related to domain effects.[21] On the high field side of the FMR mode we observe a very broad resonance feature which is due to sample edge effects, where a localized spin wave mode is excited at the sample edges.[22] Evidently there are some strong uniaxial effects which will be related to growth induced inhomogeneities in the sample.

After annealing to 350 °C for 1 h, a new resonance line is present in the FMR spectrum. This corresponds to the partially crystallized Fe phase. Further annealing shows the growth of the Fe phase resonance at the expense of that for the amorphous phase. The latter of which shifts to higher fields and decreases in intensity and is no longer evident in the spectrum corresponding to the sample after annealing to 475 °C. This is indicative of the weakening of the amorphous phase ferromagnetism, which is due to the relaxation of the amorphous structure. After annealing at 600 °C, a new resonance feature is evidenced on the high-field side of the Fe resonance line. This is due to the initial stages of second crystallization, and is related to a FeZr phase.[23–25] This resonance becomes more prominent with further annealing and shifts to lower fields which is indicated by arrows in Figs. 2(a) and 2(b). This resonance is very broad, which is indicative of significant inhomogeneity and spread of crystalline axes. In Fig. 2(a), the spectrum from the sample annealed at 650 °C, we also observe another very broad resonance in the 3000 Oe region which is due to the crystallization of other FeZr and FeB phases, see Refs. 5 and 24 and also Sec. IV C. A full discussion of the positional changes of the resonance fields of the various phases will be given in the following section.

IV. DISCUSSION

From the FMR spectra taken in the $\phi=0°$ and 90° directions we obtain the resonance field positions for the different resonances of the different ferromagnetic phases. These are plotted in Fig. 3. The inset shows an expanded view of the resonance field position for the Fe phase FMR line in both the 0° and 90° directions (filled and open circles, respectively). The variation of the amorphous phase resonance is indicative of a reduction of magnetization, as explained from the relaxation of the amorphous structure with thermal annealing. This is true for both the resonances for the amorphous phase in the 90° spectra, where both absorption peaks display a proportionate decrease of intensity and shift in field. The origin of the upper resonance mode of the amorphous phase is a localized spin wave mode at the sample edges (this has been discussed in Ref. 22). AQ denotes the as-quenched values. This represents a drop of magnetization from about 360 G in the as-quenched state to 290 G after annealing to 425 °C (we have used a value of $g=2$ to estimate the amorphous phase magnetization).

It is clear that, in general, this system consists of a multiphase magnetic material (with the exception of the as-quenched state, where the sample behaves as a single ferromagnetic amorphous phase). Therefore, it is necessary to set up the relevant resonance equations to account for the different magnetic phases and the magnetic exchange coupling that exists between them.

In the early stages of crystallization an α-Fe phase begins to form in ultrafine grains. These grains increase in size with subsequent annealing.[5] In the partially crystallized state, the samples consist of an amorphous phase magnetically coupled to the Fe nanocrystallites. This system should thus be treated as a two-phase ferromagnetic material. Furthermore, due to the confined nature of the Fe phase, we should allow for the possible excitation of standing spin wave resonance modes. A consideration of these conditions leads to a resonance equation of the form[18]

$$\begin{aligned}&\{(P_A+D_Ak_A^2)(Q_A+D_Ak_A^2)-\Omega_A^2\}\{P_BQ_B-\Omega_B^2\}\\&\quad+K_{AB}\{[(P_A+D_Ak_A^2)+(Q_A+D_Ak_A^2)][P_BQ_B-\Omega_B^2]\\&\quad+[P_B+Q_B][(P_A+D_Ak_A^2)(Q_A+D_Ak_A^2)-\Omega_A^2]\}\\&\quad+K_{AB}^2\{(P_A+P_B+D_Ak_A^2)(Q_A+Q_B+D_Ak_A^2)\\&\quad-(\Omega_A+\Omega_B)^2\}=0,\end{aligned}\tag{1}$$

where

$$\begin{aligned}P_A=V_A\{&M_AH[\sin\vartheta_A\sin\Theta_H\cos(\Phi_H-\phi_A)\\&+\cos\vartheta_A\cos\Theta_H]+2K_A^u\sin^2\vartheta_A\\&\times(\sin^2\phi_A-\cos^2\phi_A)\},\end{aligned}\tag{2}$$

$$\begin{aligned}Q_A=V_A\{&M_AH[\sin\vartheta_A\sin\Theta_H\cos(\Phi_H-\phi_A)\\&+\cos\vartheta_A\cos\Theta_H]+4\pi M_A^2(\sin^2\vartheta_A-\cos^2\vartheta_A)\\&+2K_A^u\cos^2\phi_A(\cos^2\vartheta_A-\sin^2\vartheta_A)\},\end{aligned}\tag{3}$$

$$\Omega_A=\frac{\omega}{\gamma_A}V_AM_A\sin\vartheta_A,\tag{4}$$

where K_{AB} represents the coupling strength between two magnetic phases A and B, as defined from the exchange coupling energy per unit volume as

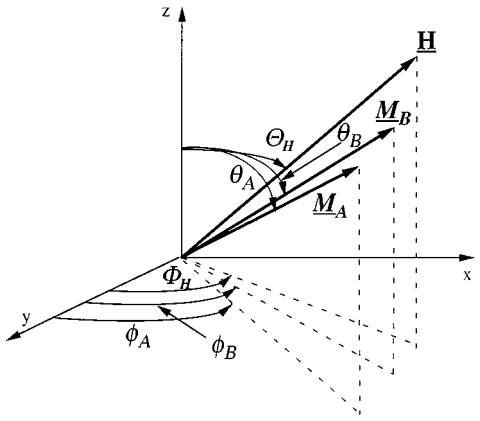

FIG. 4. Coordinate system, defining the orientations of the magnetization vectors, for a two phase system, and of the external applied field.

$$E_{AB} = -K_{AB}\frac{\mathbf{M}_A \cdot \mathbf{M}_B}{M_A M_B}. \tag{5}$$

The corresponding relations for the B terms are given by substituting B for A in the subscripts of Eqs. (2)–(4). In these expressions V_A, which is a dimensionless quantity, represents the relative volume of phase A, K_A^u represents the uniaxial anisotropy constant, γ_A is the magnetogyric ratio for this phase, M_A its magnetization, and ω represents the frequency of the microwave field. Note that for the two phase system

$$V_A + V_B = 1. \tag{6}$$

The angles ϑ and ϕ, used in Eqs. (2)–(5) are defined in Fig. 4.

In Eq. (1) we have accounted for the existence of standing spin wave resonance modes in phase A (which will represent the Fe nanocrystalline phase). Here D_A is the spin wave constant, where $D = 2A_{\mathrm{ex}}/M$, A_{ex} being the exchange stiffness constant, and k is the spin wave vector. We have not included spin wave terms for phase **B** (which will correspond to the remaining amorphous matrix). Expressions (2) and (3) are much simplified by imposing the conditions for in-plane geometry.

To analyze the data we shall define three annealing temperature regimes. The first will be for the sample where we observe the high-field resonance corresponding to the amorphous phase and the Fe phase resonance line. This corresponds to the annealing temperature range $350\,^{\circ}\mathrm{C} < T_{\mathrm{ann}} < 475\,^{\circ}\mathrm{C}$. (We exclude the as-quenched state, since this acts as a single magnetic phase.) The second regime is taken in the annealing temperature interval $425\,^{\circ}\mathrm{C} < T_{\mathrm{ann}} < 600\,^{\circ}\mathrm{C}$, the overlap with the first temperature regime will be explained in due course. The final range is from 600 to 650 °C, where FeZr phases appear, at the initial stages of the second crystallization process and later iron borides.

A. Early stages of crystallization

In the first stages of the Fe crystallization, there are two very clear and well separated resonance absorption peaks. These correspond to the amorphous phase (in the region of 2000 Oe) and the Fe phase (650–770 Oe), see Figs. 2 and 3. The large separation of the resonances reflects the distinctness of the magnetic properties of the two magnetic phases. From the as-quenched (AQ) state we calculate a magnetization (using $g = 2$) of around 360 G. Fe has a much greater magnetization in the bulk state $M = 1714$ G,[26] hence the corresponding resonance will be encountered at much lower fields. Since the two magnetic phases are in direct physical contact we may expect that the magnetic exchange coupling between them will cause a shift of their respective resonance field positions.

Due to the relatively low magnetization of the amorphous phase, we can assume a relatively weak effective magnetic coupling with the Fe phase. Following through the analysis of Eq. (1) and substituting for P_A. Q_A, etc., we obtain the resonance field dependence on the coupling strength for the weak ferromagnetic coupling as

$$(H_{\mathrm{res}})_A \approx H_K^A - 2\pi M_A - j_{AB} + \left\{ (2\pi M_A)^2 + j_{AB}^2 + \left(\frac{\omega}{\gamma_A}\right)^2 + 2j_{AB}[2\pi(M_A - M_B) - (H_K^A - H_K^B)] \right\}^{1/2}, \tag{7}$$

This is for the resonance field of phase A, that for phase B will be given by exchanging A subscripts for B. The anisotropy field for phase A, H_K^A, is defined as

$$H_K^A = \frac{2K_A^u}{M_A}. \tag{8}$$

In Eq. (7) we have applied the in-plane geometry, where the coupling parameter j_{AB} is defined as

$$j_{AB} = \frac{K_{AB} V_A M_A}{V_A M_A + V_B M_B} \tag{9a}$$

and the corresponding coupling parameter for phase B will be given by

$$j_{BA} = \frac{K_{AB} V_B M_B}{V_A M_A + V_B M_B}. \tag{9b}$$

Therefore we see that $j_{AB} \neq j_{BA}$, but $K_{AB} = K_{BA}$. In the analysis of these samples and the changes that occur upon annealing, care must be taken to account for the changes not only in the magnetic coupling strength, but also the magnetizations and relative volumes of both ferromagnetic phases. In Fig. 5, we show a plot of the resonance fields for the amorphous and nanocrystalline Fe phases as a function of the coupling strength K_{AB}. The lines show the theoretical calculations, using the above analysis, while the points correspond to experimental data taken at the annealing temperatures indicated. The values of the magnetization and of the relative volume of the magnetic phases both vary with the annealing treatment, as well as the coupling strength between the phases. In the calculations, we vary the volumes of both magnetic phases, as well as their respective magnetizations. So phase A (i.e., Fe) will grow at the expense of phase B (amorphous), in accordance with Eq. (6). The variations of the magnetizations have been modeled by assuming a proportionality of the volume of the phases with their bulk mag-

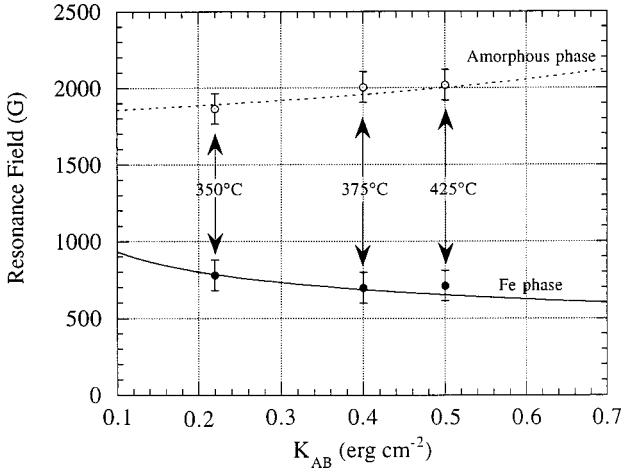

FIG. 5. Variation of the resonance field positions for the amorphous and Fe phases with exchange coupling strength K_{AB}. Points are experimental, where annealing temperatures are indicated, and lines are theoretical, see text.

netization values over the small coupling strength range given in Fig. 5. We see a fairly good agreement between theory and experiment.

It should be noted that the volumes of the phases as estimated by Mössbauer and the ferromagnetic resonance will not agree for the same annealing treatment. This is because while Mössbauer is a bulk measurement, FMR is much more sensitive to the surface of the sample, due to the skin effect,[8] where the degree of crystallization will be expected to be more developed.[27] In Ref. 27, the authors show a comparison of Mössbauer spectroscopy from the surface region (CEMS, which probes a depth of about 100 nm) and the bulk, using the conventional transmission geometry. This unequivocally shows that the crystallization in the $Fe_{81}Zr_7B_{12}$ amorphous alloy is significantly more advanced in the surface region than that of the bulk. It is fair to assume this will be the case for the present alloy under investigation. Therefore we can expect significant differences between measurements which are surface sensitive and those which are bulk measurements, for the same annealing temperature,[23] see Sec. IV F.

As the annealing temperature increases and the resonance lines move apart, the amorphous phase resonance line shifts to higher fields while the Fe phase resonance line moves to lower fields. This can be interpreted as an increase of the coupling strength with an increase of the annealing temperature (and increase of crystallization). It will be seen that the graph (Fig. 5) implies that as we increase the coupling strength, the resonance lines shift apart. This would be contrary to the intuitively expected behavior. That is, we would expect the resonance lines to approach one another as their (ferromagnetic) coupling interaction increases in strength. However, since the coupling strength will be dependent on the magnetization and on the relative quantity of the two magnetic phases, we have to be careful about how we interpret this change of coupling strength. This will be distinct from the case for magnetic multilayers where, indeed, the resonance lines of two distinct magnetic layers should approach one another as the ferromagnetic coupling strength increases. The situation here is physically different, as we are effectively changing the relative volumes of the two mag-

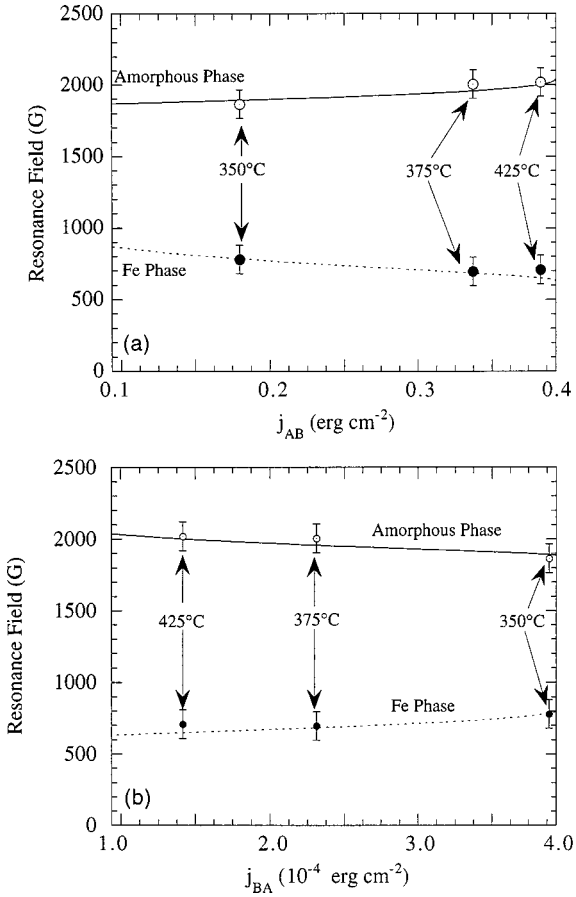

FIG. 6. Variation of the resonance field positions for the amorphous and Fe phases with exchange coupling strength for (a) the Fe phase coupling parameter j_{AB} and (b) the amorphous phase coupling parameter j_{BA}. The annealing temperatures are indicated for the experimental points.

netic phases, as well as their magnetic properties, which is generally not the case for magnetic multilayers. Clearly this situation is more complex than that for the magnetic multilayer case.

To clarify this situation we can illustrate the change of the resonance fields for the two phases as a function of the coupling parameters j_{AB} and j_{BA}, as defined in Eqs. (9a) and (9b). These are shown in Figs. 6(a) and 6(b), respectively. In Fig. 6(a), we show the variation of the resonance field of the Fe phase as a function of the Fe coupling parameter j_{AB} where the coupling parameter increases with an increase of the annealing temperature. This is as expected, since both the magnetization and the relative volume of the Fe phase will be expected to increase with annealing. In the case of the amorphous phase coupling parameter j_{BA} we see that the coupling parameter decreases with an increase of the annealing temperature (note the annealing temperatures indicated on the graph). This is due to the decrease of the relative volume of this phase, and the reduction of the effective magnetization of the remaining amorphous phase with structural relaxation.[23] The separation of the two resonance lines, and subsequent changes with increase of annealing temperature, will therefore be mainly due to the changes of the magnetization and relative volume for both ferromagnetic phases.

It should be noted that the above discussion applies only

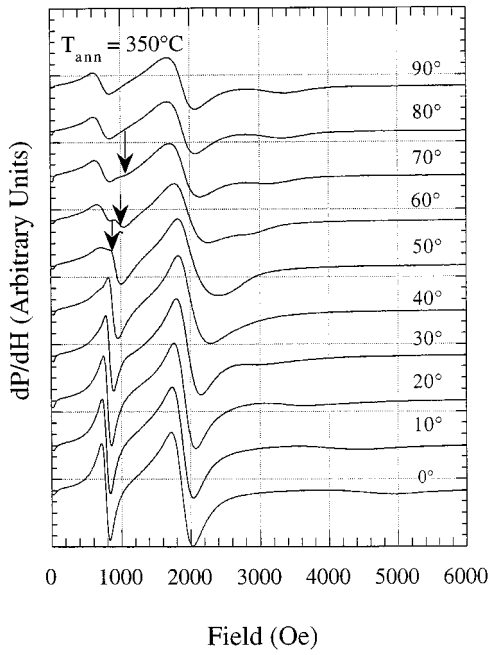

FIG. 7. Ferromagnetic resonance spectra for the sample annealed to 350 °C as a function of the angle of the applied external field, angles are labeled. Arrows show the interface localized mode at the Fe-amorphous phase boundary.

to the case of relatively weak interphase coupling. For strong coupling between two ferromagnetic phases, we would only expect a single ferromagnetic resonance mode, as will be illustrated in Sec. IV B, where the magnetic vectors for each distinct magnetic component will precess in-phase.

In Fig. 7, we show FMR spectra for the sample annealed at 350 °C, with the orientation of the applied external field in the range of $\phi = 0°$ to 90°. The general angular dependence of the low- and high-field resonance lines is discussed in Ref. 22. The two large resonance lines are due to the Fe phase (at around 750 Oe) and the ferromagnetic amorphous phase (at 1800–1900 Oe). The weak high-field resonance line is due to a spin wave resonance mode localized at the sample edges in the amorphous phase.[22] Between the Fe and amorphous phase resonance lines there is a further resonance feature (indicated by the arrows in Fig. 7, for angles $\phi = 50° - 70°$). This is due to a spin wave resonance mode localized at the interface between the Fe and amorphous phases. Due to the closeness of this resonance to the Fe resonance line at the high-field side we can deduce that this resonance is due to the Fe phase. Also, from the fact that we observe an upward shift in resonance field of this feature (with change in angle), while the FMR resonance modes (for both Fe and the amorphous phase) move down, is further evidence of the localized nature of this resonance feature.[14,22] The presence of an interface localized spin wave resonance mode is indicative of the abrupt magnetic discontinuity between the Fe phase and the weaker amorphous ferromagnetic phase.

B. Intermediate stages of crystallization

In the second temperature regime as defined above and in Fig. 3, we notice some very subtle changes in the resonance field position. Should the Fe crystallites simply continue to grow in a regular fashion, we would expect the resonance field position to exhibit a monotonic decrease, as the magnetization of the crystallites approaches that of the bulk state. In the crystallization of FeZrBCu, the segregation of the Fe forms crystallites, and leaves an Fe-rich interphase region in the amorphous matrix which surrounds the Fe crystallites.[23] This interphase can be expected to couple strongly to the Fe nanocrystalline phase, partly due to the close proximity of the two ferromagnetic phases and partly due to their relatively strong magnetizations. We can therefore use a strong coupling approximation, in which the K_{AB}^2 terms will dominate the resonance equation (1), which will give

$$\left(\frac{\omega}{\gamma_{\text{eff}}}\right)^2 = \{H\cos(\Phi_H - \phi) + H_K^{\text{eff}}(\sin^2\phi - \cos^2\phi)\} \times \{H\cos(\Phi_H - \phi) + 4\pi M_0^{\text{eff}} - H_K^{\text{eff}}\cos^2\phi\}, \tag{10}$$

where the equilibrium condition is expressed as

$$H\sin(\Phi_H - \phi) = H_K^{\text{eff}}\sin\phi\cos\phi, \tag{11}$$

where

$$H_K^{\text{eff}} = \frac{V_A M_A H_K^A + V_B M_B H_K^B}{V_A M_A + V_B M_B} \tag{12}$$

is the effective anisotropy field,

$$M_0^{\text{eff}} = \frac{V_A M_A^2 + V_B M_B^2}{V_A M_A + V_B M_B} \tag{13}$$

is the effective magnetization, and

$$\gamma_{\text{eff}} = \frac{V_A M_A + V_B M_B}{V_A M_A/\gamma_A + V_B M_B/\gamma_B} \tag{14}$$

is the effective magnetogyric ratio. It will be noted that Eq. (10) has the form of a single phase resonance equation, where the various parameters constitute an effective value, which will be an effective average of the magnetization, anisotropy field, and magnetogyric ratio for the two ferromagnetic phases. These are defined in Eqs. (12)–(14), where these average values are directly dependent on the relative volumes and magnetizations of both ferromagnetic phases. It will also be noted that the coupling strength parameter no longer enters into the resonance equation (10), as the individual magnetization vectors for the two phases are sufficiently strongly coupled that they move in-phase and effectively act as a single magnetic component. Spin wave resonance terms have been excluded from the resonance equation, because from the strong coupling between the phases at their boundaries, we will not expect a strong magnetic discontinuity, as will be found for the boundary with the amorphous phase in the early stages of crystallization. This is analogous to ferromagnetic resonance in strongly coupled magnetic layers.[28]

The equilibrium condition, Eq. (11), shows that the deviation of the magnetization vector M_0^{eff} from the direction of the applied field, which is expressed as $(\Phi_H - \phi)$, is directly dependent on the size of the effective in-plane anisotropy field. Clearly for these classes of materials, where the in-plane anisotropy is very small, these deviations of M and H

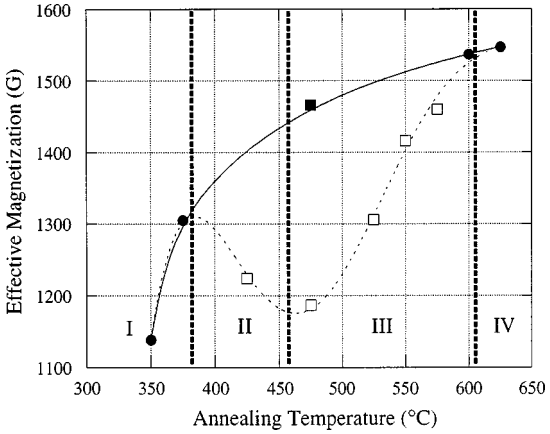

FIG. 8. Variation of the effective magnetization of the Fe phase as a function of the annealing treatment. The dashed line shows the variation for the experimental data, and the solid line the expected increase of the magnetization of the Fe crystallites for simple grain growth. Region I shows an increase of the effective magnetization in the early stages of crystallization. In region II, one sees the growth of an Fe-rich interphase in the amorphous matrix which interacts with the Fe nanocrystalline phase. This interphase region gradually crystallizes out, in region III, and disappears in region IV, returning to the expected curve of the effective magnetization of the Fe grains. See text for explanation.

will be small. At orientations of the applied external field along and across the ribbon direction (corresponding to $\phi = 0°$ and 90°, respectively), the magnetization vector will be completely aligned with the applied field. At intermediate orientations, the deviation will be small, where $\Phi_H - \phi$ is less than 0.5°.

The closeness of the magnetic properties of the α-Fe phase and the Fe-rich interphase will mean that we do not observe two clear resonance lines in the FMR spectra, and they effectively behave as one resonance. From Eq. (10) we obtain the resonance equations for the along and across ribbon directions ($\phi = 0°$ and 90°, respectively) as

$$\left(\frac{\omega}{\gamma_{\text{eff}}}\right)^2 = \{H + H_K^{\text{eff}}\}\{H + 4\pi M_0^{\text{eff}}\}$$

$$\approx \{H + H_K^{\text{eff}}\}\{H + 4\pi M_0^{\text{eff}} + H_K^{\text{eff}}\} \qquad (15a)$$

for the along ribbon direction and

$$\left(\frac{\omega}{\gamma_{\text{eff}}}\right)^2 = \{H - H_K^{\text{eff}}\}\{H + 4\pi M_0^{\text{eff}} - H_K^{\text{eff}}\} \qquad (15b)$$

for the across ribbon direction. Note that in Eq. (15a) we assume a small effective anisotropy field, this is a valid assumption in this material,[22] see Sec. IV D. From these equations, using a g factor of 2, we can estimate the effective magnetization. This is shown in Fig. 8 as a function of the annealing temperature. As the Fe crystallites grow in dimensions we would expect that the magnetization would also show an increase as the Fe becomes more bulklike. However, despite the initial increase of the magnetization from the initial annealing point at 350 °C, we observe an effective drop in magnetization upto 475 °C. This is followed by a rise in the effective magnetization. The solid line in Fig. 8 shows the expected increase of magnetization for the Fe crystallites, while the dashed line shows the variation experimentally found. The reduction of M_0^{eff}, is due to the growth of the Fe-rich interphase, which has a lower value of magnetization than Fe. (This would produce a resonance line close to that of the Fe resonance on the high-field side.) This interphase region is structurally disordered and forms an area surrounding the Fe crystallites, and includes the outer atomic layer of the Fe crystallites themselves,[23] and is distinct from the amorphous phase itself. Due to the coupling of the interphase with the Fe crystallites, we observe an apparent shift of the resonance-field position. We can now explain the variations of the effective magnetization (Fig. 8) as follows: As the interphase region grows in volume, the effective magnetization of the sample departs from the expected behavior due to the strong ferromagnetic coupling between the Fe crystallites and the interphase region. With further annealing the interphase Fe crystallite volume ratio starts to decrease, as the size of the crystallites grow, and the Fe crystallite magnetic properties will begin to dominate. This is evidenced by the increase of M_0^{eff} back towards the expected increase of the magnetization, where the solid and dashed lines gradually meet. At 600 °C the second stage of the crystallization process has commenced and the interphase region has virtually completely disappeared. We can therefore divide the crystallization of the Fe phase into four regions, indicated in Fig. 8. In region I, we have a small quantity of Fe crystallites embedded in the ferromagnetic amorphous matrix. In region II of the annealing process, an interphase region becomes evident, which has a magnetization close to but less than that of the Fe phase. This interphase, at its maximum volume at about 475 °C, forms a region of about 1 to 2 atomic layers surrounding the Fe crystallites including the outer atomic layer of the Fe crystallites themselves.[23] With further annealing, the interphase region gradually decreases in volume and starts to become crystallized, region III. This process is complete in region IV, where the interphase has virtually vanished and it has been crystallized into other crystalline phases (FeZr and Fe borides).

At the 475 °C annealing temperature we can distinguish both of the resonances from the Fe phase and the interphase, see Fig. 2(a), where these are indicated by the arrows in the 475 °C spectrum. From an approximation of the linewidth of the Fe phase we can estimate the position of the resonance field and hence its corresponding magnetization. This is indicated by the filled square in Fig. 8, and lies more or less on the solid line for the expected variation of the magnetization for the Fe crystalline phase. The existence of this interphase is in good agreement with the results of Mössbauer spectroscopy,[23] see Sec. IV F.

It will be noted that the small values of the effective magnetization, particularly in the early stages of the crystallization of the Fe phase, will be due to demagnetizing effects of the small grains. This demagnetization effect will gradually diminish as the crystallites grow and become interconnected.

C. Latter stages of crystallization

In the latter stages of the annealing range studied, a new resonance feature is observed. This is due to the beginnings of the second crystallization, where we observe the formation of a ferromagnetic phase, which is probably an FeZr crystalline phase.[24] From Fig. 2, it can be seen that this reso-

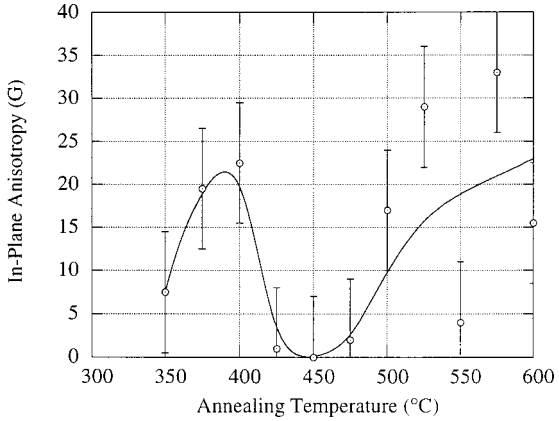

FIG. 9. Absolute value of the in-plane uniaxial anisotropy as a function of the annealing temperature.

nance feature increases in intensity and shifts to lower fields with increase of annealing temperature. This is indicated by the arrows and labeled (a). This shift down in field, with an increase of annealing temperature, is due to an increase of magnetization of this phase, while the intensity will also reflect the increase of the relative volume of this phase.

The position of the resonance field for the FeZr phase may be affected by the Fe phase due to exchange coupling effects. This would be expected to increase in importance as the FeZr phase increases in volume and magnetization. Such an effect will cause a shift of the resonance line toward that of the Fe resonance. The full analysis of changes in the coupling volume and magnetization of the FeZr phase is not given here, as we are primarily interested in the state of the sample in the region of the first crystallization, where this alloy exhibits the best soft magnetic properties. Further on in the annealing series, we observe another high-field resonance feature, just above 3000 Oe [see Fig. 2(a), spectrum for the 650 °C annealed sample, this resonance is labeled (b)], this is probably due to the crystallization of Fe_3Zr.[24,29] Using a g factor of 2, we can estimate the magnetizations of these magnetic phases, where for the 650 °C spectrum we obtain $M_1 \approx 830$ G and $M_2 \approx 60$ G. These are for room temperature measurements.

D. In-plane anisotropy

By subtracting the resonance fields in the 0° and 90° orientations, we can obtain the size of the uniaxial anisotropy field evident in these samples. Thus the anisotropy field is calculated, using Eqs. (15a) and (15b), as

$$H_K^{\text{eff}} = \frac{H_{90} - H_0}{2}, \tag{16}$$

where H_0 and H_{90} are the resonance field in the 0° and 90° directions, respectively. [Equation (16) will be valid only for small anisotropies. This is a valid assumption in the present study.] The measured in-plane anisotropy is plotted as a function of the annealing temperature in Fig. 9. This represents the anisotropy in the Fe phase only. There is a clear minimum in the region of annealing temperatures from 450 to 500 °C. This coincides with the best observed soft magnetic properties for this alloy,[30] and with the maximum quantity of the interphase. With the completion of the crystallization of the Fe phase, we see an increase of the in-plane uniaxial anisotropy, which further increases with the onset of the second crystallization. The large error bars in this figure arise from taking into account that a slight misalignment of the sample to coincide with the field in the sample plane, can cause uniaxial effects in the angular variation due to demagnetizing effects. It is estimated that a 1° misalignment of the external field in the sample plane can cause a uniaxial variation of about 5 G, see scale of anisotropy (Fig. 9). The in-plane anisotropy is greatly affected by the melt spinning technique, and is probably the origin of the uniaxial nature and anisotropy, evident in samples produced by this technique.[22]

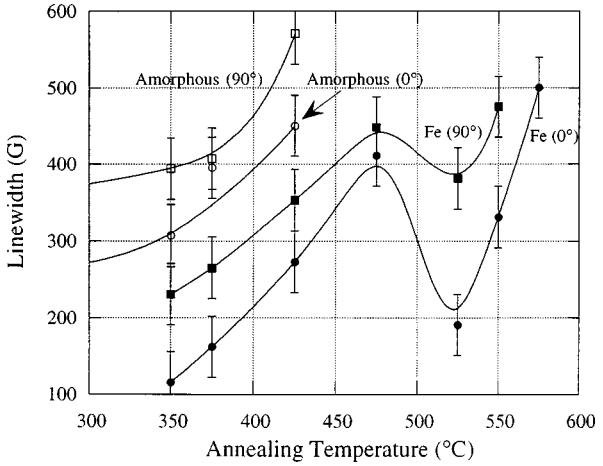

FIG. 10. Variation of the linewidths for the amorphous and Fe phases with annealing treatment.

E. Linewidth

The linewidth of resonance lines in FMR have various contributions, which are in direct relation to the state of the sample. We can represent the observed linewidth in FMR as[9–11]

$$\Delta H = \Delta H_0 + \Delta H_{\text{cryst}} + \Delta H_i, \tag{17}$$

where ΔH_0 represents the intrinsic linewidth, ΔH_{cryst} the broadening due to a variation of crystalline axes, and ΔH_i the linewidth broadening due to magnetic inhomogeneities in the sample.

The evolution of the linewidth is shown in Fig. 10 for both the amorphous and Fe nanocrystalline phases in the $\phi = 0°$ and 90° orientations. For the amorphous phase we generally observe an increase of the linewidth with annealing, which is probably due to an increase of the amorphous phase inhomogeneity during the crystallization process. For the Fe phase resonance, there is a clear maximum in the linewidth at 475 °C. This can be explained by the presence of the interphase. As the interphase grows, its resonance overlaps with that of the Fe phase, giving an apparent broadening. At 525 °C the resonance narrows, since the interphase region has virtually disappeared and there is no longer any overlap between separate resonances. Further broadening of the Fe resonance may be expected from crystallization effects, where there is a spread in the crystalline axes. This effect may be expected to be more prominent as the Fe grains increase in size.

The very broad FeZr phase resonance line (>1000 G) implies that this phase is very inhomogeneous, with a large variation of the crystalline axes and has a much larger magnetocrystalline anisotropy than the Fe phase. This large inhomogeneity may be expected from the different diffusion rates of the various components in the amorphous phase.

F. Comparison of ferromagnetic resonance and Mössbauer spectroscopy results

Despite the temperature differences expected between the results of ferromagnetic resonance and Mössbauer spectroscopy, as stated previously, there is a great deal in common between the two techniques, which is useful to outline. First, both techniques show the diminution of the amorphous phase content and the growth of the α-Fe phase, with annealing temperature. Of great significance is the observation of the Fe-rich interphase region, which surrounds the Fe crystallites. In both FMR and Mössbauer measurements, we see an agreement that this interphase region grows in relative volume, up to a certain point and then crystallizes into the various crystalline phases which subsequently form in the latter stages of the annealing temperature range studied.

By way of demonstration of the differences between the two techniques, we observe that the first evidence for the Fe-rich interphase region in the FMR experiments is found after annealing to 425 °C, whereas in Mössbauer spectroscopy, this is first noted after the annealing treatment at 475 °C. The maximum volume for the interphase is noted after annealing at 475 °C in the FMR measurements, while for the Mössbauer measurements, the maximum volume is observed after annealing at 525 °C. That is, due to the surface sensitivity of the FMR technique, the degree of crystallization in the surface region (as measured by the FMR) is similar to that in the bulk after the annealing treatment at about 50 °C above that for the FMR measurements.

In Mössbauer spectroscopy, the amorphous phase shows strong signs of becoming inhomogeneous from the hyperfine-field distribution at an annealing temperature of 475 °C. (A discussion of the Mössbauer results is given in Refs. 23 and 29 and an investigation into the temperature effects for Mössbauer spectroscopy on these materials is in progress.) This increase of inhomogeneity for the amorphous phase can be equated with the significant growth of the linewidth associated with the amorphous phase resonance at 425 °C, note the large increase of the linewidth (>150 G) from 375 to 425 °C in Fig. 10. This is supported by thermomagnetic measurements,[23] where at 475 °C we observe a strong broadening of the ferromagnetic-paramagnetic transition, which is indicative of a spread of Curie temperature values, i.e., relating to the increased inhomogeneity.

V. CONCLUSIONS

The FeZrCuB alloys present a very interesting magnetic system with regard to ferromagnetic resonance. The devitrified state of the sample, produced by thermal annealing, gives rise to various magnetic phases. The results show that we can explain the variation of the resonance lines in terms of the changes of the volumes and magnetic properties of the ferromagnetic phases present. The magnetic coupling between different magnetic phases is also shown to be of great importance.

In the early stages of crystallization the FMR spectra show two resonance lines in the ribbon direction. These are due to the ferromagnetic amorphous phase and nanocrystallites of Fe. The changes in resonance field with crystallization are related to the changes of the volumes, magnetizations, and the magnetic exchange coupling between the two phases. Changes in the Fe phase resonance, at annealing temperatures above 400 °C, are seen to be due to the presence of an Fe-rich interphase surrounding the Fe crystallites. These subtle changes in resonance field can only be explained in terms of a multiphase system. This shows the importance of the approach used here. The strong magnetic coupling between the Fe phase and the interphase (Fe-rich interphase around the Fe crystallites) means that these phases effectively act as a common single ferromagnetic phase, where the various parameters are effectively an average of the two phases present. The changes are then explained as a variation of the various parameters and the relative volumes of the phases. Results indicate that the Fe-rich interphase initially grows in volume, up to about $T_{\mathrm{ann}} \sim 475$ °C, and then gradually crystallizes into the Fe and other crystalline phases. The Fe-rich interphase zone completely disappears after annealing to 600 °C. The variation of the linewidth of the Fe resonance is consistent with the growth and subsequent crystallization of an Fe-rich interphase, with an increase of annealing temperature. The results are in agreement with Mössbauer experiments, which also show evidence for the interphase zone between the crystallites and the amorphous phase,[31] see also Refs. 6, 7, 32, and 33.

In the latter stages of the annealing range studied, we enter the second crystallization process, where we observe new resonance absorption peaks from FeZr and iron-boride phases. These resonances are very broad, indicative of a high degree of magnetic inhomogeneity in these phases.

In the sample annealed to 350 °C, we see evidence of an interface localized spin wave resonance mode. This arises from the strong magnetic discontinuity at the boundary between the amorphous matrix and the Fe nanocrystallites.

The variation of the in-plane uniaxial anisotropy shows a minimum in the annealing temperature interval 450–500 °C. This coincides with the softest magnetic properties of this alloy, where the Fe-rich interphase zone has its greatest volume.

In summary, we see that ferromagnetic resonance is a very sensitive magnetic measurement, which can reveal much about the state of partially crystallized amorphous alloys. This is a powerful complement to other structural and magnetic measurements. It is furthermore noted that it is, in general, necessary to use a multiphase approach to interpret ferromagnetic resonance measurements in these types of samples.

ACKNOWLEDGMENTS

This work was supported by the Spanish CICYT, under Grant No. MAT96/1023. Two of the authors, D.S.S. and J.S.G., would like to thank the Basque Government for financial support. We would also like to Dr. P. Gorria (University of Oviedo) and Dr. L. Fernández Barquin (University of Cantabria) for preparation of the amorphous ribbons.

*Present address: Laboratoire de Magnétisme et d'Optique—CNRS. Université de Versailles, 45 Avenue des Etats-Unis, 78035 Versailles, France.

[1] G. Herzer, Phys. Scr. **T49**, 307 (1989).

[2] G. Herzer, IEEE Trans. Magn. **25**, 3327 (1989).

[3] Y. Yoshizawa, S. Oguma, and K. Yamauchi, J. Appl. Phys. **64**, 6044 (1988).

[4] P. Gorria, J. S. Garitaonandia, and J. M. Barandiarán, J. Phys.: Condens. Matter **8**, 5925 (1996).

[5] E. Estevez-Rams, J. Fidler, M. Dahlgren, R. Grössinger, M. Knobel, P. Tiberto, P. Allia, and F. Vinai, J. Phys. D **29**, 848 (1996).

[6] M. Miglierini and J.-M. Greneche, J. Phys.: Condens. Matter **9**, 2303 (1997).

[7] M. Miglierini and J.-M. Greneche, J. Phys.: Condens. Matter **9**, 2321 (1997).

[8] S. V. Vonsovskii, *Ferromagnetic Resonance* (Pergamon, Oxford, 1966).

[9] C. Vittoria, R. C. Barker, and A. Yelon, Phys. Rev. Lett. **19**, 792 (1967).

[10] H. Yamazaki, Y. Ajiro, I. Moritani, N. Nakayama, and T. Shinjo, J. Phys. Soc. Jpn. **57**, 4343 (1988).

[11] V. Seshu Bai, S. M. Bhagat, R. Krishnan, and M. Seddat, J. Magn. Magn. Mater. **147**, 97 (1995).

[12] P. E. Wigen, Thin Solid Films **114**, 135 (1984).

[13] A. Z. Maksymowicz, Phys. Rev. B **33**, 6045 (1986).

[14] H. Puszkarski, Prog. Surf. Sci. **9**, 191 (1979).

[15] H. Bosse and H. Gärtner, J. Magn. Magn. Mater. **80**, 339 (1989).

[16] Z. Zhang, L. Zhou, P. E. Wigen, and K. Ounadjela, Phys. Rev. B **50**, 6094 (1994).

[17] D. S. Schmool, J. S. S. Whiting, A. Chambers, and E. A. Wilinska, J. Magn. Magn. Mater. **131**, 385 (1994).

[18] D. S. Schmool and J. M. Barandiarán, J. Phys.: Condens. Matter (to be published).

[19] S. N. Kaul and C. V. Mahon, J. Appl. Phys. **71**, 6090 (1992); **71**, 6103 (1992).

[20] V. Siruguri and S. N. Kaul, J. Phys.: Condens. Matter **8**, 4545 (1996); **8**, 4567 (1996).

[21] D. S. Schmool, J. S. Garitaonandia, P. Gorria, and J. M. Barandiarán (unpublished).

[22] D. S. Schmool and J. M. Barandiarán, J. Magn. Magn. Mater. (to be published).

[23] J. S. Garitaonandia, D. S. Schmool, and J. M. Barandiarán, preceding paper, Phys. Rev. B **58**, 12147 (1998).

[24] I. Navarro Palma, Ph.D. thesis, Universidad Complutense de Madrid, 1994.

[25] P. Duhaj, I. Mat'ko, P. Svec, J. Sitec, and D. Janickovic, Mater. Sci. Eng. B **39**, 208 (1996).

[26] B. D. Cullity, *Introduction to Magnetic Materials* (Addison-Wesley, New York, 1972).

[27] M. Kopcewicz and A. Grabias, J. Appl. Phys. **80**, 3422 (1996).

[28] A. Layadi and J. O. Artman, J. Magn. Magn. Mater. **92**, 143 (1990).

[29] J. S. Garitaonandia, Ph.D. thesis, Universidad del Pais Vasco, Bilbao, 1998.

[30] A. Slawska-Waniewska and J. M. Greneche, Phys. Rev. B **56**, R8491 (1997).

[31] K. Suzuki, A. Makino, A. Inoue, and T. Masumoto, J. Appl. Phys. **70**, 6232 (1991).

[32] A. Slawska-Waniewska, R. Zuberek, and P. Nowicki, J. Magn. Magn. Mater. **157-158**, 147 (1996).

[33] A. Slawska-Waniewska, R. Zuberek, J. Gonzalez, and H. Szymczak (unpublished).